

Principle Component Motion Analysis

Leif Wesche

2-1-2018

Abstract:

Principle component analysis was used to reconstruct the three dimensional motion of a spring mass system recorded from multiple two dimensional cameras. This was done by developing and implementing an algorithm that tracked the mass throughout the frames of each video, combining the tracked coordinates from each video in each test into a single data set, decomposing the data set using singular value decomposition, and analyzing the singular value spectrum and principle component projections of the data sets. It was found that as predicted, the dominant principle component of each test modeled the oscillatory motion of the mass, the next two principle components corresponded to the movement of the mass in the transverse plane, and the remaining components represented noise in the data.

I. Introduction and Overview

In this assignment, Principle Component Analysis was used to analyze an objects motion through 3 dimensional space. The object consisted of a paint can oscillating while suspended from a spring. Four tests were conducted. In the first test the paint oscillated nearly straight up and down in the z direction, in the second test the motion was similar to the first test except the camera was shaken to simulate noise. In the third test the can oscillated in both the up and down z direction but also transversely in the x-y plane, and in the fourth test the can was spun in addition to oscillating in the x, y, and z directions. Each of the four tests were recorded by three different cameras at various positions and orientations, resulting in a total of 12 videos. In each video the trajectory of the bucket was tracked in a unique reference frame. The total motion of the bucket in each test was analyzed and reconstructed using principle component analysis, or PCA.

II. Theoretical Background

Singular value decomposition is a method of PCA which decomposes a matrix A into U , V , and S components, in the form of $A = USV^T$. The U and V matrices are two separate unitary bases that can be thought of as the "ideal" reference frame to view the data matrix A . The singular value decomposition method was practical for the case of motion analysis because of the fact that the U and V bases generated by the SVD algorithm are orthogonal. Representing motion of an object through three dimensional space is most often done using a reference frame of orthogonal x, y, and z axis directions. This means that the three principle components corresponding the the three highest singular values can be thought of as representing the motion of the mass in "ideal" x, y, any z directions.

This reference frame is said to be "ideal" because the SVD algorithm seeks to represent a matrix using a least square fitting algorithm. The SVD algorithm seeks to find a new subspace with the minimum 2-norm distance between the space described by the rows of A . In other words, the algorithm aims to represent a data set most completely using the minimum number of principle components possible. In terms of the application discussed in this paper, describing three dimensional motion of a mass through space, this least squares fit feature of the SVD algorithm combined with the fact that these principle components are described using orthogonal bases is practical because this means that as complete a picture as possible of the full motion of the mass will be represented in the first principle components of the data set. This is the key that allows us to assume that the first three principle components of the matrix represent spacial quantities that are relevant to the motion of the mass in question.

III. Algorithm Implementation and Development

The function of the first and second sections of the algorithm was to load the videos into Matlab, convert the videos to into double precision numbers, and organize the videos into cells based on their specific test and camera number. The videos were also converted to gray scale for ease of processing and tracking.

A flashlight was attached to the top of the bucket, resulting in a cluster of pixels with maximum brightness at the top of the bucket. This collection of bright pixels was the distinctive characteristic of the bucket that was tracked through the course of each video. The tracking algorithm worked by searching a single frame for all of the brightest pixel positions, restraining those positions to a user specified box around the previously recorded flashlight position, searching the next box, and repeating this process until the video ended. Two sets of parameters were hand selected for each video, the dimensions and position of the initial search box, and the dimensions of subsequent search boxes. These parameters were saved in section three.

The Tracking algorithm was implemented in section four. The algorithm worked for each video by finding the x-y coordinates of all the pixels with the brightest points in a single frame, then computing the average x-y position of the bright cluster. Next, using the initial search box parameters, any x or y positions that were outside the box were discarded. The average of the remaining x and y points were calculated, rounded to the nearest whole value, and recorded as the object position in that frame. A search box for the next frame was constructed by adding and subtracting by adding fixed lower and upper bounds to the x and y coordinates of the points identified in the last frame. A new point was found within the new search box, and the cycle repeated until the end of each recording. Figure 1 below shows an example of a frame with the search box and flashlight position plotted on top of it.



Figure 1: Example frame showing the selected point (red) and the constraining search box (blue).

In section 5, the data was aligned and centered. The multiple recordings of each test did not start simultaneously, meaning that the x and y positions tracked had to be aligned in time by cropping the x and y vectors. The motion of the can was nearly ideally periodic in all directions, so to align the videos the x and y position vectors were plotted and cropped so that all of the data sets began while the paint can was at its lowest point in the vertical direction. The x and y position vectors for each test were then arranged row wise into a single 6 row matrix for each test, since there were 3 recording of each test and two dimensional measurements from each recording, x and y. Four test matrices were constructed in total.

The x and y data in each row of the matrices were then centered so that the data could all be compared at the same reference magnitude. The position vectors were recorded from videos that did not share any common positions or orientations, so the locations tracked were not centered around a common axis. This lack of consistency would negatively effect the outcome of the PCA analysis, thus aligning the tracked positions was necessary. This was done by taking the average of each row of position data and subtracting it from every point.

The purpose of section 6 was simply to plot the cropped and aligned position data that would be analyzed using PCA. Some of these plots can be seen in Figures 2 and 3.

In section 7 the principle components of each of the four test matrices were analyzed using PCA, specifically singular value decomposition. This was easily done using Matlab's SVD command with the economy setting enabled. First the singular values for each test matrix were plotted and analyzed to determine the number of degrees of freedom of the spring mass system in each test. A plot of the singular value spectrum normalized by the sum of the values can be seen in Figure 5.

Next, principle components were calculated by projecting the test matrices onto their respective U bases. The principle components pertaining to the spacial dependencies of the mass were calculated by multiplying $U^T * A = S * V^T$. The four projections can be seen in Figure 6.

IV. Computational Results

The tracking algorithm in Section 4 worked well for most of the tests. The first of the tests was most successfully tracked. In this test, the can moved nearly exclusively in the vertical direction with little transverse movement and a stable camera. Figure 2 shows the X and Y coordinates tracked from each recording of test 1.

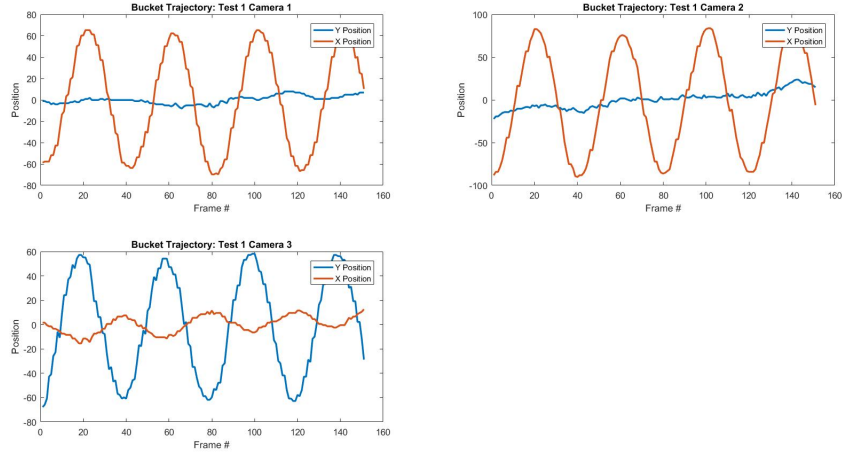


Figure 2: Test 1 Bucket Trajectory.

Test 3 was the most difficult to track. In test 3 the bucket moved nearly only in the vertical direction, just as it did in test 1, except noise was introduced to the data in the form of camera shake. The testing algorithm had varying success with these tests, even after several different sets of input parameters were tested. However, despite the noise, oscillatory motion could be observed from the measurements. Figure 3 below shows the motion of the bucket measured from test 3.

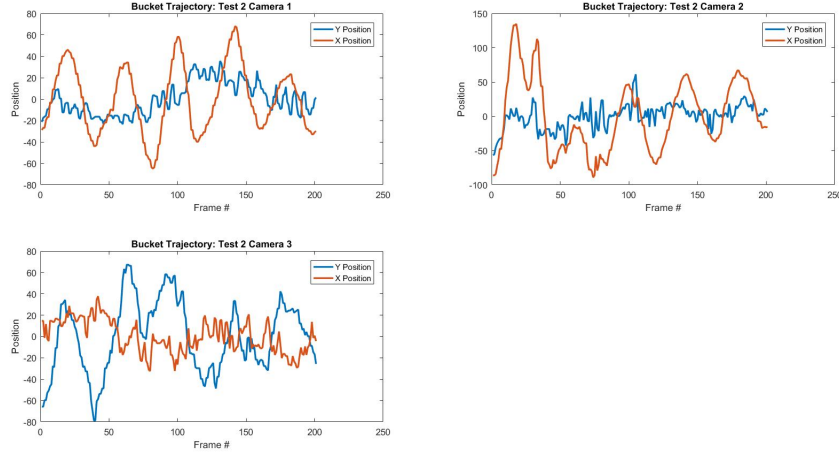


Figure 3: Test 2 Bucket Trajectory.

Tests 3 and 4 both yielded similar results from the tracking algorithm. In test 3, the bucket was released off center which resulted in movement in the horizontal plane as well as in the vertical direction. The bucket was also released off center in test 4, but now the bucket was spun as it was released which resulted in rotational motion as well as motion in all three directions. The bucket was tracked fairly well in both tests, but occasionally the cameras lost sight of the flashlight on top of the bucket, in which case the software tracked a different part of the white bucket. The rotation did not appear to significantly change the effects of the motion tracking. Figure 4 below shows the results of tracking the bucket in test 3, and Figure ?? in Appendix A shows the results of tracking test 4.

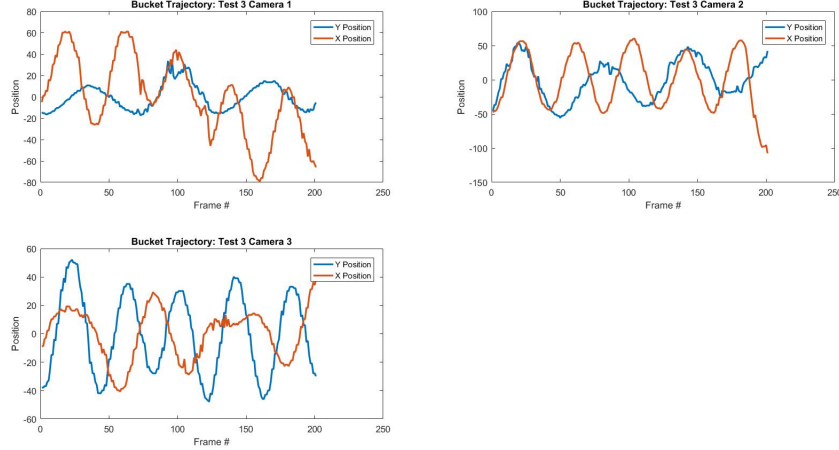


Figure 4: Test 3 Bucket Trajectory.

In section 7, the data sets for each of the four tests were decomposed into U, S, and V components. First, the singular values, or the components of the diagonal matrix S, were analyzed to determine the significance of each principle component. There were 6 singular values total corresponding to 6 sets of position data for each test. In each test, the mass was moved through three spacial dimensions to varying degrees. This means that the expected result was that the first three singular values would correspond to movement in spacial coordinates, while the next values correspond to noise. The expected result was that the first singular value would be much higher than the others for every test, since the motion of the can was primarily up and down in every test. The singular values were normalized by their sum and plotted. The plots are shown below in Figure 5.

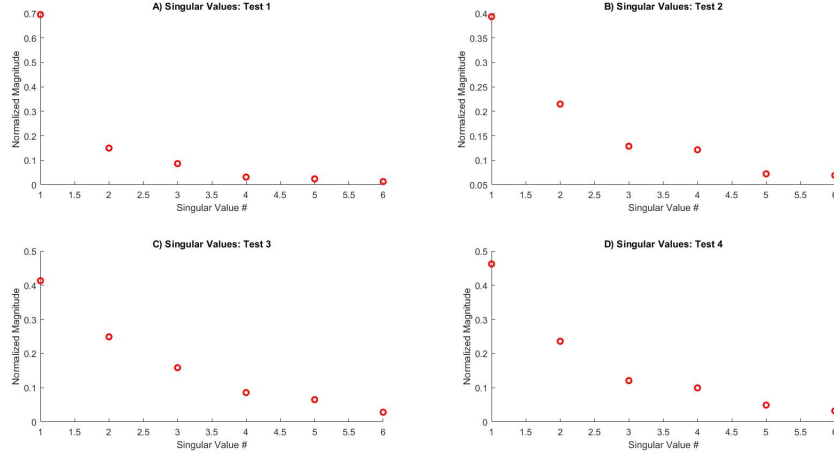


Figure 5: Singular value spectrums of all four tests.

In each test, the first singular value was by far larger than the others, which fits the expected result. In test one, shown in Figure 5a the first value made up 70% of the total singular value spectrum. In this test, the motion was primarily only in the vertical direction, so the expected result is very small singular values for the next two values, which was seen in the data. The next two singular values are much smaller than the first one, each around 10% of the total sum, and the following three values were very small, around 2%. Test 1 fit the expected results.

The singular values for test 2 are shown in Figure 5b. The first singular value made up around 40% of the sum of the spectrum. This value is smaller than in the case of test 1, and this difference is attributed to the effects of increased noise and instability. The next singular value is around 25%, and the third and fourth values are very close together around 15%. This would imply that although there are only really three dimensions the can is moving in, the excess noise in test 2 made it difficult to discern the third dimension of motion from noise.

The singular values for tests 3 and 4 are shown in Figures 5c and 5d respectively. The singular values for both cases were very close, showing that the rotation of the can did little to change the outcome of the tests. This makes sense, since the tracking algorithm only tracked the mass of the can as a whole through space, not its rotation. The singular values fit the expected results, with the first value being much higher than the rest. The highest singular values from tests 3 and 4 were slightly larger than that of test 2, but not as high as test one, which makes sense. In tests 3 and 4, the can moved in the transverse direction, as well as up and down. This means that if tracked accurately, singular values two and three in test 3 and 4 should be higher than the singular values two and three in test 1, which they were. In the case of test 3 and 4, the larger second and third singular values correspond to transverse motion that was absent in test 1.

The motion of the paint can in each of the principle component directions was also calculated by projecting the test data onto the matrix U , the first orthogonal base created by the SVD algorithm. This was done for each test by computing $U^T * Data$, analogous to the expression $S * V^T$, where $Data$ represents the position data in the x and y coordinates of each video for a single test. The results of this projection in the first three principle directions are shown below in Figure 6.

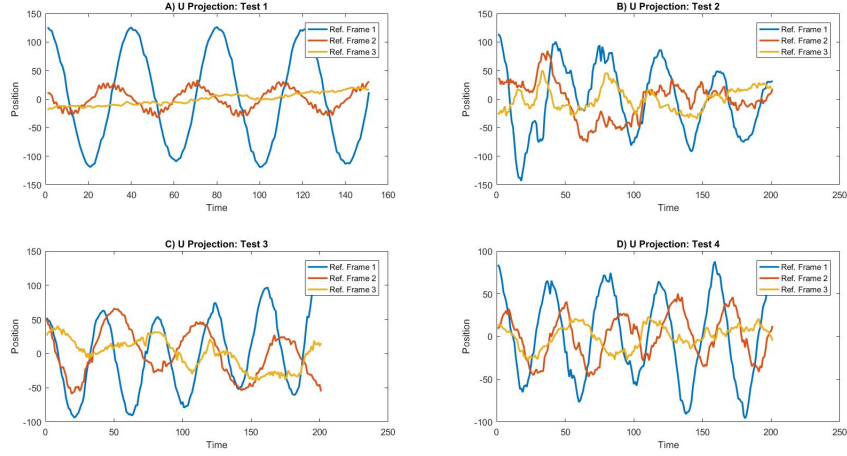


Figure 6: Projection of the test data onto the orthogonal bases U .

Figure 6a shows the motion of the mass in test 1 in the ideal coordinates calculated by the SVD algorithm. The oscillations of test 1 was almost completely in the vertical direction, which is what is seen in the projection. There is also a small movement in another direction, which can be seen in the red line in 6a. This small movement in a transverse direction can be observed in the recordings of test 1. Principle component analysis effectively separated the movement of test 1 into orthogonal bases which corresponded directly to the coordinate system that is intuitively optimal for the spring mass case.

The projection of the test 2 position data onto its corresponding base U was a less clear picture of the motion, but despite the noise and camera shake, the oscillatory motion of the mass is still visible in the projection. While noise is prominent in the image, the blue line shown in Figure 6b clearly shows the expected sine wave like oscillatory motion, corresponding to the vertical motion of the mass.

The motion of test 3 and 4 represented in their first three principle components, shown in Figures 6c and 6d, also clearly show oscillatory motion in their first principle component. Similarly, oscillatory motion can also be observed in the second and third principle components of tests 3 and 4, which fits the expected results, since the mass in these tests was moving a significant amount in the transverse direction as well as in the vertical direction. The rotation of the can in test 4 seemed to have little effect on the end result, except for perhaps resulting in slightly noisier data due to the fact that the tracking algorithm likely had a harder time tracking a rotating object accurately.

The 3 lowest singular components are shown in Figure ?? in Appendix A. These additional principle components are typically much smaller in magnitude in tests 1, 3, and 4, which fits the expected result, since these components should correspond to noise instead of any real motion. The three final principle components for test 2, however, are much larger due to the additional noise in these videos. Still, the vertical oscillatory motion of the mass represented by the first principle component is clear in all tests.

V. Summary and Conclusions

Principle component analysis was used to analyze the motion of a mass at the end of a spring mass system using data recorded from three different cameras over four separate tests. An algorithm was used to track the mass through each frame of each recording, and sets of x-y position data was recorded from each camera's reference frame. These x-y positions were assembled into one data matrix for each test, and each data matrix was decomposed using singular value decomposition. The singular value spectrum was analyzed for each test to determine the significance of each principle component, and the test data was projected onto the orthogonal bases produced by the SVD algorithm to observe how the mass moved in its ideal reference frame. As predicted, oscillatory motion was the largest principle component observed in each test. Thus, the largest principle component corresponded to the vertical motion mass spring system, and the total movement of the mass was described from the videos using principle component analysis.